On the turbulent sources of the solar dynamo

V. V. Pipin
Institute for Solar-Terrestrial Physics
Siberian Division of the Russian Academy of Sciences
664003 Irkutsk, RUSSIA
e-mail address: pip@iszf.irk.ru

N. Seehafer
Institut für Physik und Astronomie,
Universität Potsdam,
Karl-Liebknecht-Str. 24/25
14476 Potsdam-Golm, GERMANY
e-mail address: seehafer@uni-potsdam.de

Abstract

We revisit the possible turbulent sources of the solar dynamo. Studying axisymmetric mean-field dynamo models, we find that the large-scale poloidal magnetic field could be generated not only by the famous α effect, but also by the $\mathbf{\Omega}\times\mathbf{J}$ and shear-current effects. The inclusion of these additional turbulent sources alleviates several of the known problems of solar mean-field dynamo models.

1 Introduction

Most solar dynamo models use the scenario proposed by Parker [3]. In this scenario, the solar magnetic field is produced by an interplay between differential rotation and the collective action of cyclonic turbulent convection flows. The latter is widely known as the α effect [2], which is believed to be responsible for the generation of the poloidal component of the large-scale magnetic field (LSMF) of the Sun. There are, however, a number of problems with the α effect [1], and recent developments of mean-field magnetohydrodynamics have stimulated a quest for additional or alternative turbulent dynamo mechanisms. The influence of turbulence on the evolution of the LSMF is expressed by the mean electromotive force (MEMF) $\boldsymbol{\mathcal{E}} = \langle \mathbf{u}\times\mathbf{b}\rangle$, where $\mathbf{u}$ and $\mathbf{b}$ are the fluctuating parts of the velocity and magnetic field (angular brackets denote ensemble averages). It can be written in compact form as

$$\boldsymbol{\mathcal{E}} = (\hat{\alpha}+\hat{\gamma})\circ\mathbf{B} - \left(\hat{\eta}+\hat{\Omega}+\hat{W}+\ldots\right)\circ(\nabla\times\mathbf{B})\,. \tag{1}$$

Here $\mathbf{B}$ is the mean, large-scale magnetic field. The tensors $\hat{\alpha}$, $\hat{\gamma}$ and $\hat{\eta}$ describe the α effect, turbulent pumping and turbulent diffusion, $\hat{\Omega}$ the $\mathbf{\Omega}\times\mathbf{J}$ effect (or $\delta^{(\Omega)}$ effect) and $\hat{W}$ the shear-current effect (or $\delta^{(W)}$ effect). Discussions of the different contributions to $\boldsymbol{\mathcal{E}}$ may, for instance, be found in [6, 7]. In this paper, we use calculations of them as described in [4], and construct a set of axisymmetric kinematic dynamo models in a convective spherical shell. These models are obtained as solutions of the mean-field dynamo equation

$$\frac{\partial\mathbf{B}}{\partial t} = \nabla\times(\mathbf{V}\times\mathbf{B}+\boldsymbol{\mathcal{E}})\,, \tag{2}$$

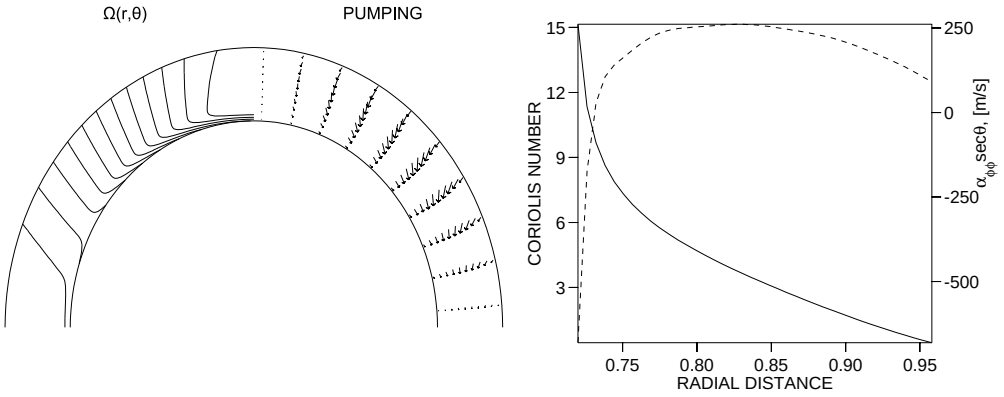

Figure 1: Basic model quantities. Left panel: Contours of the rotation rate in the solar convection zone (left) and geometry of the pumping velocity of the toroidal LSMF (right); the maximum amplitude of the pumping velocity is about 1 m/s. Right panel: Radial profiles of the Coriolis number Ω^* (solid line) and $\alpha_{\phi\phi}\sec\theta$ (dashed line). $\alpha_{\phi\phi}$ changes sign near the bottom of convection zone. Similar radial dependences are found for the other components of the $\hat{\alpha}$ tensor.

where $\mathbf{V} = r\sin\theta\,\Omega\,(r,\theta)$, with $\Omega(r,\theta)$ modeling the differential angular rotation rate of the Sun (r and θ denote radius and colatitude); see Fig. 1, left-hand side in left panel. The LSMF is modeled in the form $\mathbf{B} = \mathbf{e}_\phi B\,(r,\theta) + \nabla\times\left(\dfrac{A\,(r,\theta)\,\mathbf{e}_\phi}{r\sin\theta}\right)$ ($\mathbf{e}_\phi$ denotes the azimuthal unit vector), and the MEMF is calculated according to Eq. (1). Details of the procedure are given in [5]. The radial profiles of characteristic quantities of the turbulence, such as the rms convective velocity u_c, the correlation length and time ℓ_c and τ_c, and the density stratification parameter $G = \nabla\log\rho$ (ρ is the mass density), are computed on the basis of a standard model of the solar interior [8]. Some of the generation effects depend on the rms intensity of a fluctuating background magnetic field $\mathbf{b}^{(0)}$, generated by a small-scale dynamo. We assume energy equipartition between $\mathbf{b}^{(0)}$ and the turbulent velocity field, i.e. $\sqrt{\left\langle {\mathbf{b}^{(0)}}^2\right\rangle}/\left(u_c\sqrt{4\pi\rho}\right) = 1$. The relative strengths of the turbulence effects are controlled via parameters C_α (α effect), C_ω ($\mathbf{\Omega}\times\mathbf{J}$ effect) and C_W (shear-current effect); in addition, turbulent pumping is always present, depending merely on the turbulence level (with which all other contributions are also scaled). The integration domain is radially bounded by $r = 0.71R_\odot$ and $r = 0.96R_\odot$, where the boundary conditions are $\dfrac{\partial rB}{\partial r} = 0, A = 0$ at the bottom boundary, and vacuum conditions at the top boundary. Four basic model quantities, namely, the differential rotation, the turbulent pumping velocity of the toroidal component of the LSMF and the radial profiles of the Coriolis number $\Omega^* = 2\Omega_0\tau_c$ ($\Omega_0 = 2.86\cdot10^{-6}s^{-1}$ is the surface rotation rate) and of $\alpha_{\phi\phi}\sec\theta$ ($\alpha_{\phi\phi}$ measures the strength of the azimuthal α effect) are shown in Fig. 1.

2 Results

We now discuss examples of dynamos obtained by combining the α effect with the $\mathbf{\Omega}\times\mathbf{J}$ and shear-current effects. It was found earlier [9] that for solar conditions and without meridional circulation, $\delta^{(\Omega)}\Omega$ dynamos ($\mathbf{\Omega}\times\mathbf{J}$ effect plus differential rotation) have steady non-oscillatory dynamo eigenmodes. We found that the same applies to $\delta^{(W)}\Omega$ dynamos (shear-current effect plus differential rotation) and to combinations of $\delta^{(\Omega)}\Omega$ and $\delta^{(W)}\Omega$ dynamos. This means that the α effect is needed in solar dynamo models, at least in

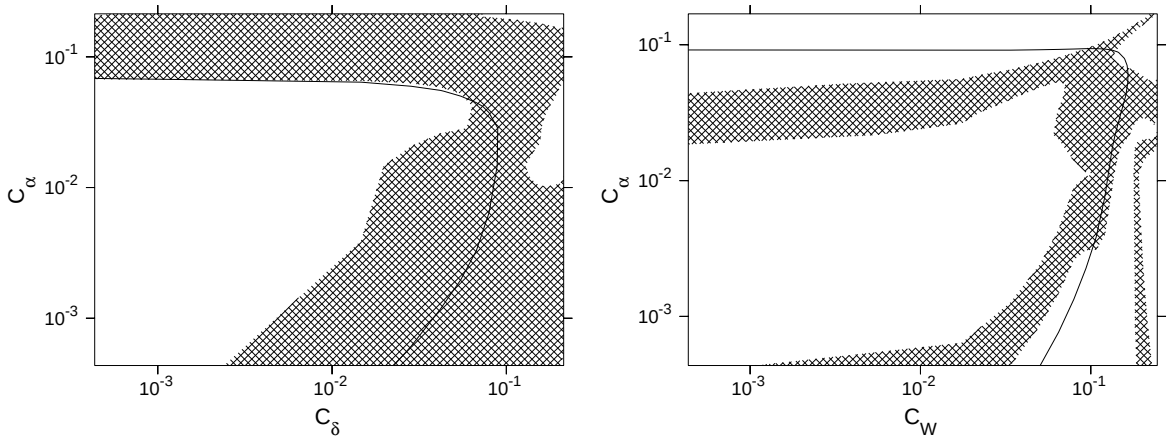

Figure 2: Stability diagrams for the $\alpha^2\delta^{(\Omega)}\Omega$ (left panel) and $\alpha^2\delta^{(W)}\Omega$ (right panel) dynamos. The stable regions (no dynamo) lie below and to the left of the solid lines. Shading indicates dominance of dipole modes.

such without meridional circulation. Fig. 2 gives stability diagrams for $\alpha^2\delta^{(\Omega)}\Omega$ and $\alpha^2\delta^{(W)}\Omega$ dynamos, which include the usual $\alpha^2\Omega$ dynamo as a limiting case. As is seen in Fig. 2, in this latter case the dipole modes are not the most unstable modes. Fig. 3 shows snapshots of the evolution of the LSMF in the $\alpha^2\Omega$ dynamo and the associated butterfly diagram, obtained from the first unstable dipole eigenmode. We assume that the sunspot activity is produced by the toroidal LSMF in the whole convection zone and have integrated the toroidal field over radius. The obtained dynamo has some similarity with the observed evolution of the large-scale magnetic activity of the Sun, e.g., the "correct" phase relation between the toroidal and poloidal components — the polar reversal of the radial component of the LSMF takes place when the amplitude of the toroidal component passes its maximum, and the toroidal fields drift towards the equator in the course of the activity cycle. There are a number of problems, however. Two of them are: (i) The period of the activity cycle is $T \lesssim 1\,\mathrm{yr}$ (corresponding to about 0.1 turbulent diffusion times), which is much shorter than the observed period of 22 yr. (ii) The activity maxima are found at mid latitudes, rather than, as observed, at low latitudes.

The inclusion of the two additional turbulent generation mechanisms of the poloidal LSMF reduces the frequency of the dynamo wave. Fig. 4 demonstrates this for the example of an $\alpha^2\delta^{(\Omega)}\Omega$ dynamo. Oscillatory modes are excited if C_α is not very small compared to C_ω. In the range $1 < C_\omega/C_\alpha < 3$ the match with the solar observations is best. As can be seen in Fig. 2, the dipole modes are the primary dynamo modes in this parameter interval. While the wings of the obtained dynamo waves are too wide, other qualitative properties, such as the drift directions of the toroidal and poloidal components of the LSMF and their phase relation, are reproduced correctly. The period of the dynamo in this parameter range is shorter than but comparable with the turbulent diffusion time.

Our last example is a dynamo where the poloidal LSMF is built up with the help of the shear-current effect. Fig. 5 shows the time evolution of the LSMF and the associated butterfly diagram for an $\alpha^2\delta^{(W)}\Omega$ dynamo model. Some properties of the model agree well with the observations. For example, the period of the dynamo waves is comparable with the turbulent diffusion time. Also, the maximum amplitudes of the toroidal component of the LSMF are found below 30° latitude, and this field component drifts towards the equator during the cycle. A very unwelcome issue of the model, however, is that the maxima of the radial component of the LSMF are also concentrated near the equator.

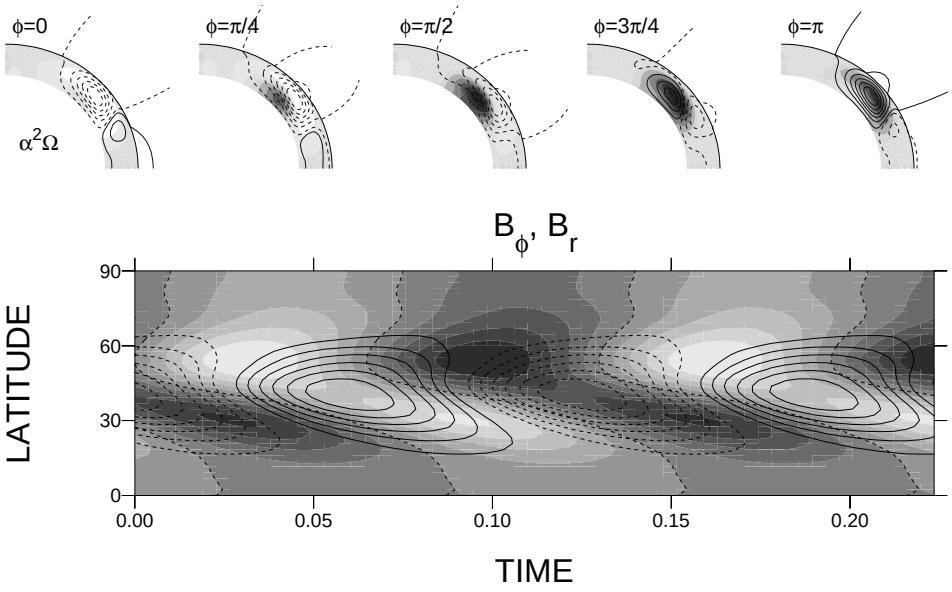

Figure 3: $\alpha^2\Omega$ model on the basis of the first unstable dipole eigenmode. Top: Snapshots of the strength of the toroidal LSMF (greyscale plot) and field lines of the poloidal LSMF over an half cycle. Bottom: Butterfly diagram in the form of contour lines of the toroidal LSMF (integrated over radius) with overlaid greyscale plot for the radial LSMF at the top boundary. Time is measured in units of the turbulent diffusion time.

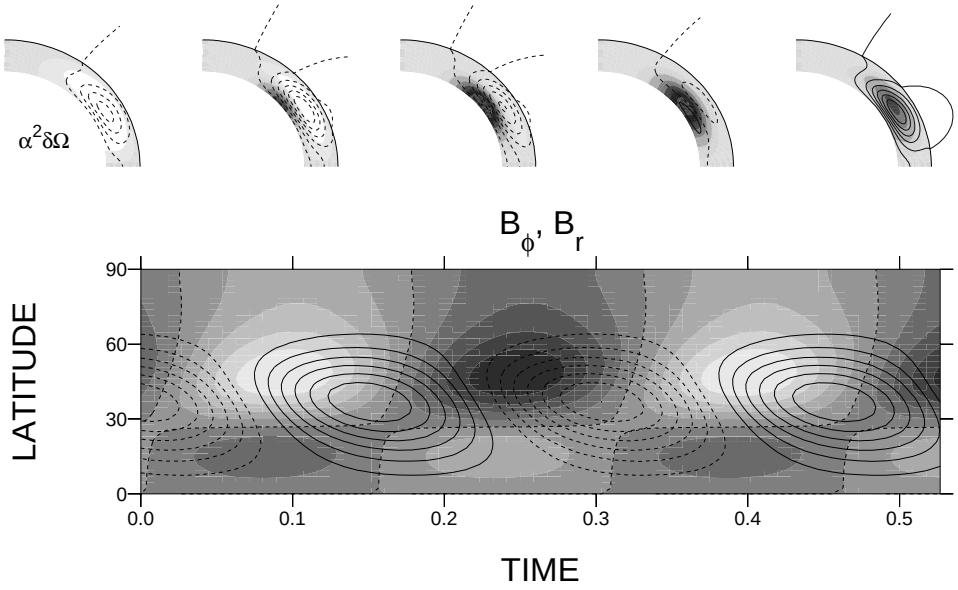

Figure 4: As Figure 3, but for the $\alpha^2\delta^{(\Omega)}\Omega$ model with $C_\omega = 0.1$, $C_\alpha = 0.05$.

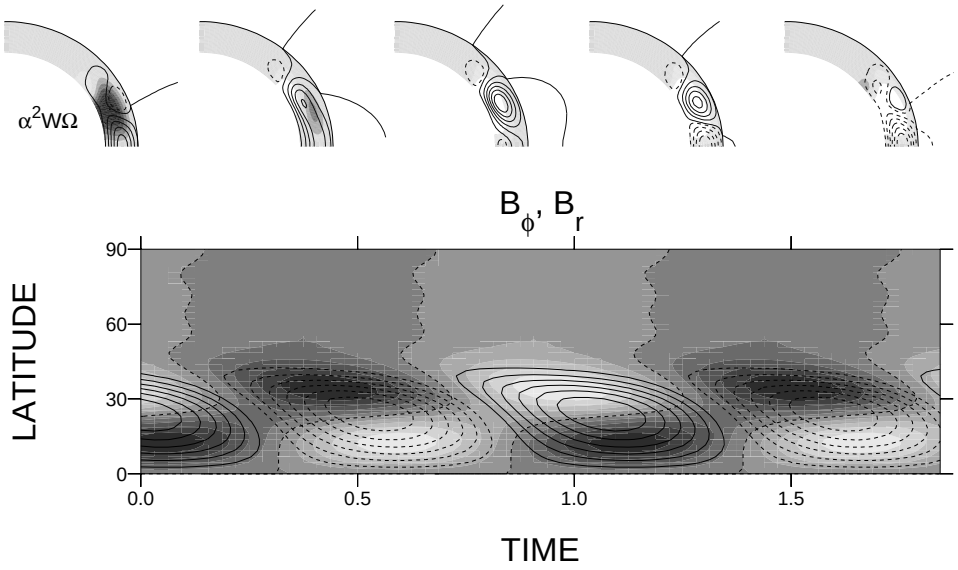

Figure 5: As Figure 3, but for the $\alpha^2\delta^{(W)}\Omega$ model with $C_W = 0.1$, $C_\alpha = 0.01$.

3 Conclusions

The inclusion of the $\mathbf{\Omega} \times \mathbf{J}$ and shear-current effects in addition to the α effect and differential rotation in axisymmetric kinematic dynamo models alleviates some of the known problems of current mean-field solar dynamo models. For instance, the simulated period of the dynamo is increased and comes, thus, closer to the observed activity period. Furthermore, the large-scale toroidal field is concentrated towards the equator, thus bringing the models in better agreement with the observation of two activity belts relatively close to the equator. Improved diagnostic tools based on both observation and theory are needed to clarify the roles of the different turbulence effects, as well as that of meridional circulation, which was not included in the present study.

References

[1] Brandenburg, A.; Subramanian, K.: Astrophysical magnetic fields and nonlinear dynamo theory. Phys. Rep. 417 (2005) 1–209.

[2] Krause, F.; Rädler, K.-H.: Mean-Field Magnetohydrodynamics and Dynamo Theory. Berlin: Akademie-Verlag 1980.

[3] Parker, E. N.: Hydromagnetic dynamo models. Astrophys. J. 122 (1955) 293–314.

[4] Pipin, V. V.: The mean electro-motive force and current helicity under the influence of rotation, magnetic field and shear. Geophys. Astrophys. Fluid Dynam. 102 (2008) 21–49.

[5] Pipin, V. V.; Seehafer, N.: Stellar dynamos with $\mathbf{\Omega} \times \mathbf{J}$ effect. Astron. Astrophys. In Press

[6] Rädler, K.-H.; Stepanov, R.: Mean electromotive force due to turbulence of a conducting fluid in the presence of a mean flow. Phys. Rev. E 73 (2006) 056311.

[7] Rogachevskii, I.; Kleeorin, N.: Nonlinear theory of a "shear-current" effect and mean-field magnetic dynamos. Phys. Rev. E 70 (2004) 046310.

[8] Stix, M.: The Sun. An Introduction. Berlin: Springer 2002, 2nd edition.

[9] Stix, M.: Differential rotation and the solar dynamo. Astron. Astrophys. 47 (1976) 243–254.